

# 1 Modelling the permeability loss of metallic iron water filtration systems

2 Caré S.<sup>(a)</sup>, Crane R.<sup>(b)</sup>, Calabrò P.S.<sup>(c)</sup>, Ghauch A.<sup>(d)</sup>, Temgoua E.<sup>(e)</sup>, Noubactep C.<sup>(f,g)\*</sup>

3 <sup>(a)</sup> Université Paris Est, Laboratoire Navier (ENPC/IFSTTAR/CNRS), 2 allée Kepler, F- 77420 Champs sur  
4 Marne, France (sabine.care@ifsttar.fr).

5 <sup>(b)</sup> Interface Analysis Centre, University of Bristol, 121 St. Michael's Hill, Bristol, BS2 8BS, UK.  
6 (Richard.Crane@bristol.ac.uk)

7 <sup>(c)</sup> Università degli Studi Mediterranea di Reggio Calabria, MECMAT, Mechanics and Materials Department,  
8 Faculty of Engineering, Via Graziella, loc. Feo di Vito, 89122 Reggio Calabria, Italy. (paolo.calabro@unirc.it)

9 <sup>(d)</sup> American University of Beirut, Faculty of Arts and Sciences, Department of Chemistry, P.O. Box 11-0236  
10 Riad El Solh-1107-2020 Beirut, Lebanon. (ag23@aub.edu.lb)

11 <sup>(e)</sup> University of Dschang, Faculty of Agronomy and Agricultural Science, P.O. Box 222 Dschang, Cameroon.  
12 (emile.temgoua@univ-dschang.com)

13 <sup>(f)</sup> Angewandte Geologie, Universität Göttingen, Goldschmidtstraße 3, D - 37077 Göttingen, Germany.

14 <sup>(g)</sup> Kultur und Nachhaltige Entwicklung CDD e.V., Postfach 1502, D - 37005 Göttingen, Germany.

15 Correspond author; e-mail: cnoubac@gwdg.de; Tel. +49 551 39 3191, Fax. +49 551 399379

## 17 Abstract

18 Over the past 30 years the literature has burgeoned with in-situ approaches for groundwater  
19 remediation. Of the methods currently available, the use of metallic iron ( $\text{Fe}^0$ ) in permeable  
20 reactive barrier (PRB) systems is one of the most commonly applied. Despite such interest, an  
21 increasing amount of experimental and field observations have reported inconsistent  $\text{Fe}^0$   
22 barrier operation compared to contemporary theory. In the current work, a critical review of  
23 the physical chemistry of aqueous  $\text{Fe}^0$  corrosion in porous media is presented. Subsequent  
24 implications for the design of  $\text{Fe}^0$  filtration systems are modelled. The results suggest that: (i)  
25 for the pH range of natural waters ( $> 4.5$ ), the high volumetric expansion of  $\text{Fe}^0$  during  
26 oxidation and precipitation dictates that  $\text{Fe}^0$  should be mixed with a non-expansive material;  
27 (ii) naturally-occurring solute precipitates have a negligible impact on permeability loss  
28 compared to  $\text{Fe}^0$  expansive corrosion; and (iii) the proliferation of  $\text{H}_2$  metabolising bacteria

29 may contribute to alleviate permeability loss. As a consequence, it is suggested that more  
30 emphasis must be placed on future work with regard to considering the Fe<sup>0</sup> PRB system as a  
31 physical (size-exclusion) water filter device.

32 **Keywords:** Deep-bed filtration, Hydraulic conductivity, Modelling, Permeability loss,  
33 Zerovalent iron.

#### 34 **Acronym List**

35 ITRC Interstate Technology & Regulatory Council

36 PRB Permeable reactive barrier

37 RZ Reactive Zone

38 ZVI Zerovalent iron

39

#### 40 **1 Introduction**

41 Permeable reactive barriers containing metallic iron as a reactive filler material (Fe<sup>0</sup> PRBs) is  
42 an established technology for groundwater remediation [1-10]. At present, more than 120 Fe<sup>0</sup>  
43 PRBs have been installed worldwide, and effective performance has typically been reported  
44 [10-13]. Fe<sup>0</sup> PRBs typically contain either pure Fe<sup>0</sup> or a mixture of Fe<sup>0</sup> and another material,  
45 such as gravel or sand. The incorporation of a secondary material is typically employed either  
46 to meet design requirements, cost, or to limit permeability loss. In such cases, potential  
47 drawbacks on the kinetics of contaminant removal must be considered [14]. However, some  
48 available experimental results from batch [15,16] and column [14,17] studies suggest that  
49 admixing pumice/sand to Fe<sup>0</sup> is beneficial for the process of contaminant removal. Therefore,  
50 the recent statement of Ulsamer [13] that “there is no conclusive evidence that a sand/iron mix  
51 is better or worse than a pure iron barrier” can be considered the current state-of-the-art.

52 In addition, the challenge of determining the fundamental mechanisms which govern  
53 hydraulic conductivity (permeability) loss is yet to be properly addressed [10,11,13,18,19]. At  
54 present it is suggested that the mechanism of permeability loss in Fe<sup>0</sup> PRBs is due to the

55 accumulation of insoluble minerals within the PRB pore network [10,13]. Relevant minerals  
56 include siderite ( $\text{FeCO}_3$ ), aragonite ( $\text{CaCO}_3$ ), and iron (hydr)oxides (e.g.  $\text{Fe}(\text{OH})_2$ ,  $\text{Fe}(\text{OH})_3$ ,  
57  $\text{FeOOH}$ ,  $\text{Fe}_2\text{O}_3$ ,  $\text{Fe}_3\text{O}_4$ ) [10,13,20-26]. Another mechanism reported attributes the  
58 permeability loss to the build-up of  $\text{H}_2$  gas, formed due to the hydrolysis of water during  $\text{Fe}^0$   
59 corrosion [11,27,28]. However, as  $\text{H}_2$  is a key source of energy for numerous different  
60 microorganism species [23,29-31], the contribution of  $\text{H}_2$  to the process of  $\text{Fe}^0$  PRB  
61 permeability loss has been ascribed as minor [32].

62 The theory that  $\text{Fe}^0$  PRB permeability loss is predominantly due to the accumulation of  
63 insoluble minerals within pore volumes was recently challenged by Henderson and Demond  
64 [11]. The authors cited that whilst natural groundwater constituents (e.g. carbonates) and  
65 contaminant species can occur in subsurface concentrations of several hundred parts per  
66 million (or mg per litre), the mass/volume occupied by the mineral precipitates will be minor  
67 compared to the large amount required to significantly impair the permeability of an average  
68 permeable reactive barrier system. Based on this premise they attributed the permeability loss  
69 to the accumulation of  $\text{H}_2$  gas, and suggested periodical venting to prevent build-up. All  
70 studies to date, however, have overlooked the role of the volumetric expansive iron corrosion  
71 products [33-36] in PRB permeability loss.

72 In the current work, a multidisciplinary theoretical approach has been applied to analyse the  
73 relationship between the extent of  $\text{Fe}^0$  depletion and permeability loss in  $\text{Fe}^0$  beds (including  
74 water filters and PRBs), by linking: contemporary knowledge of the mechanisms which  
75 govern contaminant removal by  $\text{Fe}^0$  [37]; with mathematical modelling mass conservation  
76 equations. Much of the impetus for this work originates from recent work summarized in  
77 Noubactep et al. [38] wherein the advantages of admixing non-expansive materials to  $\text{Fe}^0$   
78 within  $\text{Fe}^0$  filtration systems are discussed. For the sake of clarity, the basic conservation  
79 equation for the oxidative dissolution of iron will be given.

80 **2 Conservation equation of iron corrosion at pH > 4.5**

## 81 **2.1 Basic conservation equation**

82 The basic constitutive equation expressing the overall conservation of mass of any chemical  
83 element (j) consumed in a chemical reaction relates volume (V), dry bulk density ( $\rho$ ), and  
84 chemical composition (C) and mass fluxes (m) into or out of a system [39]:

$$85 \quad V_p \rho_p C_{j,p}/100 + m_{j,\text{flux}} = V_w \rho_w C_{j,w}/100 \quad (1)$$

86 The first term of Eq. 1 expresses the mass of element j, contained in the original material  
87 before reaction, subscripted as p. It is given by the product of volume (V in  $\text{cm}^3$ ), dry bulk  
88 density ( $\rho$  in  $\text{g}/\text{cm}^3$ ), and elemental concentration (C in weight %). The mass of element j  
89 introduced into or out of the considered volume is indicated as  $m_{j,\text{flux}}$  and is added to the mass  
90 of j in the system. Fluxes ( $m_{j,\text{flux}}$ ) are positive if they enter the system and negative if they exit  
91 the system. On the right-hand side of Eq. 1, the mass of element j contained in the volume of  
92 reaction products, subscripted w, is given by the product of the new volume, dry bulk density,  
93 and element concentration.

## 94 **2.2 Conservation equation of iron corrosion at pH > 4.5**

95 For iron corrosion, the element of concern is iron ( $j = \text{Fe}$ ) which is distributed between the  
96 original metallic iron ( $\text{Fe}^0 = \text{ZVI}$ ) and various iron hydroxides and oxides ( $w = \text{ox}$ ). Eq. 1 can  
97 therefore be written as:

$$98 \quad V_{\text{ZVI}} \rho_{\text{ZVI}} C_{\text{Fe,ZVI}} + m_{\text{Fe,flux}} = V_{\text{ox}} \rho_{\text{ox}} C_{\text{Fe,ox}} \quad (2)$$

99 For pH > 4.5 the solubility of iron is very low and the flux of Fe ( $m_{\text{Fe,flux}}$ ) can be largely  
100 neglected assuming that water flow rate is slow enough that the dissolution/precipitation  
101 reactions are at pseudo-equilibrium. Eq. 2 can be re-written as:

$$102 \quad V_{\text{ZVI}} \rho_{\text{ZVI}} C_{\text{Fe,ZVI}} = V_{\text{ox}} \rho_{\text{ox}} C_{\text{Fe,ox}} \quad (2a)$$

103 Eq. 2a suggests that  $V_{\text{ox}}$  (iron oxide) must be larger than  $V_{\text{Fe}}$  (metallic iron) because all iron  
104 (hydr)oxides are less dense than  $\text{Fe}^0$  (Tab. 1).

## 105 **2.3 Volumetric strain**

106 With regard to iron corrosion driven volume changes, there are three possibilities: (i)  
107 volumetric compression ( $V_{ZVI} > V_{ox}$ ), (ii) isovolumetric transformation ( $V_{ZVI} = V_{ox}$ ), and (iii)  
108 volumetric expansion ( $V_{ZVI} < V_{ox}$ ). Accordingly, volumetric changes should be determined  
109 experimentally. This is accomplished by using the classical definition of strain,  $\epsilon$ , the ratio of  
110 volume change in a process to the initial volume (Eq. 3):

$$111 \quad \epsilon = (V_{ox} - V_{ZVI})/V_{ZVI} = (V_{ox}/V_{ZVI}) - 1 \quad (3)$$

112 Eq. 3 suggests that the volumetric strain is positive because  $V_{ox}/V_{ZVI} \geq 2.1$  [35].

113 In the next section, a new approach for the discussion of permeability loss will be given. This  
114 exercise will be based on the recent paper by Henderson and Demond [11].

### 115 **3 Permeability loss in Fe<sup>0</sup>/H<sub>2</sub>O systems**

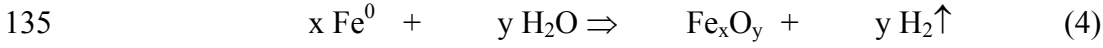
116 The purpose of this section is to discuss the relative importance of mineral precipitation, gas  
117 production and expansive iron corrosion for permeability loss in Fe<sup>0</sup>/H<sub>2</sub>O systems. Expansive  
118 iron corrosion products included rust. To this end, the species discussed by Henderson and  
119 Demond [11] will be considered individually (Table 1).

120 A cylindrical column apparatus for Fe<sup>0</sup> filtration has an internal diameter (D), a reactive  
121 length ( $H_{rz}$ ), and a subsequent total volume  $V_{rz}$  ( $V_{rz} = \pi \cdot D^2 \cdot H_{rz} / 4$ ).  $H_{rz}$  may be a fraction of  
122 the length of the column apparatus ( $H_{rz} \leq H$ ). A column may also contain several reactive  
123 zones. The discussion herein is limited to a single reactive zone. The ratio of the initial  
124 volume of the void space (inter-particle porosity) is  $\Phi_0$  and the volume of pore is  $V_p =$   
125  $\Phi_0 \cdot V_{rz}$ . The volume occupied by the solid particles  $V_{solid}$  is  $V_{solid} = (1 - \Phi_0) \cdot V_{rz}$ . Solid  
126 particles include Fe<sup>0</sup> and additives (e.g. gravel, pumice, sand), assumingly having the same  
127 size and shape (roundness or sphericity). The following cylindrical column apparatus used by  
128 Henderson and Demond [11] is considered:  $D = 5$  cm,  $H_{rz} = H = 25$  cm, a subsequent  $V_{rz} =$   
129  $491.1$  cm<sup>3</sup>, and initial porosities ( $\Phi_0$ ) of 0.62.  $\Phi_0 = 0.62$  is also from ref. [11].

130 The challenge of the current work is to evaluate which quantity of each fouling species (iron  
 131 corrosion products) is necessary to occupy the initial pore volume ( $V_p$ ).

### 132 **3.1 Filling the pore volume with individual minerals and $H_2$ gas**

133 In this section, Eq. (4) assumes that  $Fe^0$  is oxidized by water. The initial pore volume ( $V_p$ ) is  
 134 filled entirely by corrosion products ( $H_2$  and  $Fe^{II}/Fe^{III}$  species):



136	$t_0 = 0$	$n_0$	0	0
137	$t > t_0$	$n_0^*(1 - \alpha)$	$n_0^*\alpha/x$	$y*n_0^*\alpha/x$
138	$t > t_0$	$x*n'_0*(1 - \alpha)$	$\alpha*n'_0$	$y*n'_0*\alpha$

139 It is considered that the number of moles ( $n_0$ ) of  $Fe^0$  at time  $t = 0$  ( $t_0$ ) is a multiple of  $n'_0$  ( $n_0 =$   
 140  $x*n'_0$ ). Accordingly, at  $t_0$ , the reactive zone contains only  $x*n'_0$   $Fe^0$  (no oxide and no  
 141 hydrogen). At each time  $t$  ( $t > t_0$ ), the residual number of moles of  $Fe^0$  is  $x*n'_0*(1 - \alpha)$ , the  
 142 number of mole of generated oxide is  $\alpha*n_0/x = \alpha*n'_0$  and the number of mole of  $H_2$  is  
 143  $y*n_0*\alpha/x = y*n'_0*\alpha$  where  $\alpha$  is the fraction of the initial amount of  $Fe^0$  which is depleted as a  
 144 function of time ( $t$ ). For iron hydroxides ( $Fe(OH)_n$ ) and carbonate ( $FeCO_3$ ), the stoichiometry  
 145 of oxygen is taken as the value of “ $x$ ” ( $y = x$ ) because each mole of Fe releases one mole of  
 146  $H_2$  (for  $n = 2$ ).

147 Knowing the molar volume of individual oxides and  $H_2$  (Tab. 1), the degree of occupation of  
 148 the initial pore volume ( $V_p$ ) can be evaluated. The reactive zone is clogged when enough  
 149 corrosion products ( $Fe_xO_y$  and  $H_2$ ) are produced to completely fill  $V_p$ . In other words, bed  
 150 clogging corresponds to Eq. (5):

$$151 \quad V_{ZVI} + V_{ox} + V_{H_2} = V_{rz} \quad (5)$$

152 The volume  $V_i$  occupied by a species  $i$ , is the product of its molar volume by the number of  
 153 moles. The equation of the clogging can be written as (Eq. 5a):

$$154 \quad V_{m,ZVI}*x*n'_0*(1 - \alpha) + V_{m,ox}*n'_0*\alpha + V_{m,H_2}*n'_0*y*\alpha = V_{rz} \quad (5a)$$

155 To have  $\alpha$  values for individual oxides, it is sufficient to solve Eq. 5a. The solution is given  
156 by Eq. 5b:

$$157 \quad \alpha = [V_{rz}/x * n'_0 - V_{m,ZVI}] / [V_{m,ox}/x + y/x * V_{m,H2} - V_{m,ZVI}] \quad (5b)$$

158 The porosity of granular sandy beds used in sand filters ranges from 0.40 to 0.50 (average of  
159 0.45) [41]. The porosity of the filtration bed depends on several factors including grain size,  
160 grain size distribution and shape (sphericity) of used particles [42]. The sphericity of the  
161 medium is a measure of its roundness and ranges from 0.70 (angular grains) to about 0.90  
162 (grains rounded by water or wind) [41,43].

163 The volume of  $Fe^0$  ( $V_{Fe}$ ) in the pure  $Fe^0$  system (100 %  $Fe^0$ ) depends on the compactness  $C$  or  
164 the porosity  $\Phi$  ( $V_{Fe} = C * V_{RZ} = (1 - \Phi) * V_{RZ}$ ). Reported operational values for the porosity of  
165  $Fe^0$  systems vary between 40 and 70 % [10,11,15]. Calculations are made for the extreme  
166 values of the porosity reported in peer-reviewed journal articles (36 and 62 %).  $\Phi_0 = 36$  %  
167 corresponds to the ideal case of spherical materials [38]. The initial number of moles of  $Fe^0$   
168 ( $n_0$ ) corresponding to the extreme cases are 41.4 ( $\Phi_0 = 36$  %) and 24.6 ( $\Phi_0 = 62$  %).  
169 Calculations (Tab. 2) showed that if  $H_2$  does not escape from the reactive zone, the  
170 consumption of less than 0.1 % of the initial amount of  $Fe^0$  will be sufficient to clog the  
171 systems. If this was likely to occur, the  $Fe^0$  filtration technology would have not been  
172 possible.

173 Calculations assuming total escape of  $H_2$  gas out of the reactive zone ( $V_{m,H2} = 0$  in Eq. 5b)  
174 indicate that 16 to 62 % of  $Fe^0$  can be depleted just at system clogging ( $\Phi_{t\infty} = 0$  %) when the  
175 initial porosity is 36 %. For  $\Phi_0 = 62$  %, 46 to 100 %  $Fe^0$  could be depleted just at system  
176 clogging ( $\alpha \geq 0.46$ ). In other words, the sustainability of a  $Fe^0$  filtration system depends  
177 strongly from its initial porosity ( $\Phi_0$ ).

178 The results herein suggest that, for  $\Phi_0 = 36$  %, when the main corrosion product is  $Fe_3O_4$ ,  
179 only 58 % of  $Fe^0$  is consumed just at system clogging. This value in agreement with the value

180 of 51 % reported in former works [38]. The difference corresponds to different values used  
181 for the volumetric expansion coefficient ( $\eta$ );  $\eta = 1.97$  herein vs.  $\eta = 2.08$  in ref. [37].  
182 However, this approach fails to consider the in-situ generation of colloidal  $\text{Fe}^{\text{II}}/\text{Fe}^{\text{III}}$  species  
183 and their further transformation to hydroxides and oxides [44,45].

184 Eq. 5b describes a pure iron bed (100 %  $\text{Fe}^0$ ). In the case that  $\text{Fe}^0$  is admixed with a non  
185 expansive additive (e.g. gravel, pumice, sand) the initial number of moles of iron ( $n_0$ ) has to  
186 be corrected to the fraction of  $n_0$  corresponding to the volumetric proportion of Fe in the  
187 reactive zone, e.g.  $n_0/2$  for a system containing 50 %  $\text{Fe}^0$  (v/v) and the balance amount of a  
188 non porous material.

189 The results from Tab. 2 suggest that, at  $\Phi_0 = 36$  %, pure  $\text{Fe}^0$  beds are not sustainable as a rule  
190 (see section 3.2.2). For larger initial porosity ( $\Phi_0$ ), more sustainable systems are obtained.  
191 This result was already theoretically achieved by admixing  $\text{Fe}^0$  and porous media (e.g.  
192 pumice). However, increased initial porosity as discussed here results from the geometry  
193 (size, shape) of used media (e.g.  $\text{Fe}^0$ , sand, gravel).

194 The influence of the shape of the  $\text{Fe}^0$  particles on the  $\text{Fe}^0$  bed porosity is schematically  
195 represented in Fig. 1 as spherical (left) and cylindrical (right)  $\text{Fe}^0$  particles (black) are  
196 progressively transformed to oxides (grey - rust). Fig. 1 confirms the fact that packed beds of  
197 spherical media are the most compact [46-49]. This delineates the importance of  
198 characterizing  $\text{Fe}^0$  and sand materials for their uniformity and sphericity and the resulting bed  
199 for its compactness (porosity).

200 Another important feature seen in Tab. 2 ( $\alpha$  and  $\alpha'$  values) is that regardless from the  
201 abundance of  $\text{Fe}^0$  in the system, bed clogging due to  $\text{H}_2$  gas production is likely to occur prior  
202 to the consumption of 0.1 %  $\text{Fe}^0$ . However, under the experimental conditions considered by  
203 Henderson and Demond [11], gas accumulation is unlikely since the solutions were pumped  
204 in upflow at a flow rate of 0.7 mL/min into the columns. In addition, under field conditions,



205 H<sub>2</sub> consuming bacteria are ubiquitous [29]. In such cases, clogging is therefore more likely to  
206 result from enhanced (bio-)stimulation (biofilm growth) and not from H<sub>2</sub> accumulation.  
207 The estimations in this section clearly show that if H<sub>2</sub> was primarily responsible for bed  
208 clogging, then it is unlikely that the Fe<sup>0</sup> PRB technology would have been effective on  
209 medium to long-term timescales as observed in the field. PRB clogging would have been  
210 prevalent before a fraction (less than 0.1 %) of the Fe<sup>0</sup> had corroded. However, H<sub>2</sub> gas may  
211 contribute to permeability loss in association with particle ‘cementation’ (compaction) by  
212 nascent iron hydroxides. In this case, compaction prohibits H<sub>2</sub> escape and increases flow  
213 resistance for pumped solutions.

### 214 **3.2 The process of permeability loss in Fe<sup>0</sup>/H<sub>2</sub>O systems**

215 In this section, a contemporary evaluation of permeability loss in the Fe<sup>0</sup>/H<sub>2</sub>O system is given.  
216 The methodology is explicitly presented in ref. [38]. In the current work the following  
217 assumptions apply:

- 218 (i) Uniform Fe<sup>0</sup> corrosion: the radius reduction of spherical or cylindrical Fe<sup>0</sup> particles is the  
219 same for all particles;
- 220 (ii) the volume of the reactive zone ( $V_{rz}$ ) remains constant and the volume of granular  
221 materials (e.g. sand) is not modified by the corrosion process;
- 222 (iii) Fe<sup>0</sup> corrosion products are fluid enough to progressively fill available pore space.

223 As shown in section 2.3, iron corrosion occurs with concurrent volumetric expansion ( $\eta =$   
224  $V_{ox}/V_{ZVI} > 1$ ). The excess volume of Fe<sup>0</sup> imbued by corrosion product formation is given by  
225  $V_{excess}$  in Eq. 6. By definition,  $V_{excess}$  is the difference between  $V_{ox}$  and  $V_{ZVI}$  (Eq. 6).

$$226 \quad V_{excess} = (\eta - 1) * V_{ZVI} \quad (6)$$

227 The Fe<sup>0</sup> filtration system is clogged when the volume  $V_{excess}$  is equal to the initial inter  
228 granular voids ( $V_p$ ). “ $V_{ZVI}$ ” in Eq. 6 represents the volume of Fe<sup>0</sup> in a pure Fe<sup>0</sup> bed. However,  
229 as discussed in sections 1 and 3.1, Fe<sup>0</sup> should be only a fraction of  $V_{solid}$  ( $V_{ZVI} = \tau_{ZVI} * V_{solid}$ ,  
230 with  $\tau_{ZVI} \leq 1$ ). Eq. 6 can be rewritten as:

$$231 \quad (\eta - 1) * \tau_{ZVI} * V_{\text{solid}} = V_{\text{excess}} \quad (6a)$$

232 Eq. 6a suggests that, for every  $\eta$  value (i.e. every oxide),  $V_{\text{excess}}$  is a linear function of  $\tau_{ZVI}$ . To  
 233 find out at what extent  $\tau_{ZVI}$  contributes to complete pore filling, it is sufficient to graphically  
 234 solve Eq. 6a for  $V_{\text{excess}} = V_p$ . Practically, there are two equivalent approaches: (i) solving  
 235  $V_{\text{excess}} - V_p = 0$  or (ii) solving  $V_{\text{excess}}/V_p = 1$ . The second approach is adopted in this work.  
 236 The solution of Eq. 6a (clogging) is the interception of the line  $V_{\text{excess}}/V_p = f(\tau_{ZVI})$  with the line  
 237 100 % (Fig. 2). Before discussing the actual evolution of the porosity, some fundamental  
 238 aspects for the solution of Eq. 6a will be given.

### 239 **3.2.1 Fe<sup>0</sup> filtration systems**

240 To date, Fe<sup>0</sup> particles have been widely reported as successful for water treatment [50-53].  
 241 However, a holistic understanding of the Fe<sup>0</sup>/H<sub>2</sub>O system is yet to be achieved.

242 Fig. 2 represents the principle of Fe<sup>0</sup> filtration beds. The origin (point O) represent a Fe<sup>0</sup>-free  
 243 filter (e.g. activated alumina, activated carbon, gravel, pumice, sand, zeolite) and point  
 244 I(100,100) represents an “ideal Fe<sup>0</sup>-based filter” which becomes 100 % clogged concurrent  
 245 with 100 % Fe<sup>0</sup> depletion ( $V_{\text{excess}}/V_p = 1$ ). The line OI divides the graph into two halves.  
 246 Below OI,  $V_{\text{excess}}/V_p < 100$  and the system is not clogged at Fe<sup>0</sup> depletion. Above OI,  
 247  $V_{\text{excess}}/V_p > 100$  and the system is clogged before Fe<sup>0</sup> depletion (a proportion of Fe<sup>0</sup> is  
 248 wasted). Thus, Fig. 2 can be regarded as a useful reference tool for future work within this  
 249 field. Relevant parameters to complement Fig. 2 that will be investigated in future work  
 250 include: (i) the intrinsic reactivity of Fe<sup>0</sup>; (ii) the shape and size of Fe<sup>0</sup>; (iii) the shape and size  
 251 of sand; (iv) the dimensions and the geometry of the Fe<sup>0</sup> bed; (v) the thickness of the Fe<sup>0</sup>/sand  
 252 layer; (vi) the proportion of Fe<sup>0</sup> in the Fe<sup>0</sup>/sand layer; and (vii) the water flow velocity.

253 Point O in Fig. 2 represents all filtration designs without Fe<sup>0</sup> (or another metallic element).  
 254 These include conventional slow sand filters (SSF), biosand filters (BSF) and iron oxide-  
 255 coated sand filters. Considering filtration designs which entirely contain sandy materials,  
 256 point O can be limited to BSF and SSF. SSF have been used for water treatment since 1840 in

257 Dijon/France by Henry Darcy [54]. BSF have been used for water treatment at household  
258 level for over 20 years [55,56]. However, despite intensive research on BSF, their operating  
259 mode is yet to be completely understood [42,43,55]. For example, there are no established  
260 comprehensive design criteria for BSF [41,55,57]. Accordingly, the reproducibility and  
261 comparison of reported results from one setting to another is problematic. To fill this gap,  
262 Kubare and Haarhoff [41] have provided the most recent systematic review for a rational  
263 design of BSF. A  $\text{Fe}^0$  filtration system (Fig. 2) can be regarded as a modification of a SSF or  
264 BSF (point O). Therefore, it is essential to carefully develop rational and comprehensive  
265 engineering design criteria. In this effort, designing tools for BSF would be very helpful  
266 [41,55].

### 267 **3.2.2 The role of initial porosity in $\text{Fe}^0$ bed clogging**

268 The theoretical discussion of  $\text{Fe}^0$  PRB porosity until now was focused on the case of  
269 maximum compactness for which the initial porosity is 0.36 ( $\Phi_0 = 36\%$ ) [32]. For such  
270 systems, a pure  $\text{Fe}^0$  bed is clogged when less than 60% of the initial amount of  $\text{Fe}^0$  is  
271 depleted (section 3.1). According to Fig. 1, for  $\Phi_0 = 36\%$ , all  $\text{Fe}^0$  beds are situated above line  
272 OI. However, significantly larger porosity values have typically been reported in the  
273 literature, the highest being 62% by Henderson and Demond [11]. Accordingly, this section  
274 discusses the evolution of the porosity of a conventional sand filter (0%  $\text{Fe}^0$ ) as it is  
275 progressively transformed to a pure  $\text{Fe}^0$  filter (100%  $\text{Fe}^0$ ). Particular attention is paid to the  
276 extreme values of the porosity ( $\Phi_0 = 36$  and 62%). The results are summarized in Fig. 3.

277 The ideal line OI is not represented in Fig. 3 for clarity. Instead the point I(100,100) is  
278 represented. Fig. 3a ( $\Phi_0 = 0.36$ ) shows clearly that all systems are clogged before  $\text{Fe}^0$   
279 depletion has been occurred. In contrast, Fig. 3b shows that, for an initial porosity ( $\Phi_0$ ) of  
280 0.62,  $\text{Fe}^0$  beds are sustainable if magnetite ( $\text{Fe}_3\text{O}_4$ ), maghemite ( $\gamma\text{-Fe}_2\text{O}_3$ ) and hematite  
281 ( $\text{Fe}_2\text{O}_3$ ) are the sole iron corrosion products. Additionally, it shows that ferrous hydroxide  
282 ( $\text{Fe}(\text{OH})_2$ ) is the “ideal corrosion product” for the  $\text{Fe}^0$  PRB to clog concurrent with  $\text{Fe}^0$

283 depletion. With the formation of ferrous hydroxide, magnetite, maghemite and hematite being  
284 more prevalent in anoxic conditions, it can therefore be stated that Fe<sup>0</sup> PRBs are most ideally  
285 suited for oxygen depleted or anoxic conditions.

286 Magnetite ( $x_{\text{Fe}} = 72.4 \%$ , Tab.1) may result from Fe(OH)<sub>2</sub> dehydration under anoxic  
287 conditions and is therefore the sole mineral, that is likely to be quantitatively generated from  
288 anoxic Fe<sup>0</sup> corrosion.

### 289 **3.2.3 Discussion**

290 The presentation until now has focused on the evolution of the permeability loss as a key  
291 factor for the sustainability of Fe<sup>0</sup> PRB systems. A Fe<sup>0</sup> filtration system is sustainable only if  
292 it can maintain hydraulic (permeability) performance while also remaining effective for  
293 pollutant removal. In other words, a permeable but non reactive Fe<sup>0</sup> filtration system is  
294 useless.

295 A Fe<sup>0</sup> filtration system can be considered both a chemical and physical water filter device,  
296 with its efficacy dictated by progressive expansion/compression cycles during aqueous  
297 corrosion [52]. In a Fe<sup>0</sup> filtration system, chemical reactions included (i) iron oxidative  
298 dissolution, (ii) polymerisation of iron hydroxides and, (iii) subsequent precipitation of  
299 hydroxides and oxides. Quantitative chemical transformations (oxidation/reduction) of  
300 dissolved species may also occur. However, resulted species must be removed from the  
301 aqueous phase by a physical process: adsorption, occlusion, size-exclusion. Accordingly, Fe<sup>0</sup>  
302 is not a strong reducing agent under environmental conditions as widely accepted [5-7,10].  
303 More importantly, reduction is not a stand alone contaminant removal mechanism [58-61].  
304 Rather, Fe<sup>0</sup> is a generator of contaminant scavengers for reactive filtration [44,62-65]. While  
305 adsorptive filtration has been mostly used for metal removal [62-65], the affinity of organic  
306 compounds for iron hydroxide/oxides (corrosion products) is well documented [66-71]. For  
307 example, Saha et al. [71] investigated the adsorptive removal of seven different dyes on iron

308 oxide nanoparticles are reported on enhanced adsorption capacity of the dyes containing  
309 hydroxyl (-OH) (erichrome black-T, bromophenol blue, bromocresol green, and fluorescein).  
310 For the proper scaling of Fe<sup>0</sup>-supported sand filters as reactive filtration device, factors  
311 sustaining size exclusion should be understood and optimised [72]: (i) the pore size must be  
312 small enough for sufficient contaminant removal; or (ii) used Fe<sup>0</sup> must be reactive enough to  
313 produce a sufficient amount of ‘scavengers’ as a function of time. Alternatively, the thickness  
314 of the Fe<sup>0</sup> PRB can be increased to improve the device’s filtration capacity.  
315 This highlights the importance of characterizing the intrinsic reactivity of Fe<sup>0</sup> materials prior  
316 to application [73]. Ideally, the selection of a Fe<sup>0</sup> material for a particular site should be  
317 governed by its intrinsic reactivity (and porosity when incorporated in the PRB system) and  
318 the expected impact of local geochemical (and geophysical) conditions on these factors. In  
319 cases where contaminant breakthrough was observed despite insignificant permeability loss,  
320 two explanations can be suggested: (i) the material is not reactive enough to generate  
321 “scavengers” in sufficient quantities, (ii) clogging of the entrance zone has disturbed the flow  
322 regime and preferential flow paths are created in the system. Preferential flow paths  
323 significantly impair the contact of flowing water with bed media (collectors, iron, sand).

#### 324 **4 Conclusions**

325 Correlating the fundamental relationship between Fe<sup>0</sup> PRB permeability loss and groundwater  
326 chemistry is extremely important for the design of sustainable Fe<sup>0</sup> remediation systems.  
327 Further developments require knowledge of the intrinsic reactivity of Fe<sup>0</sup>, the rate of the  
328 formation of corrosion products and the role of foreign detrital minerals. Using mathematical  
329 modelling, the present communication challenges both the prevailing view and the  
330 contribution of Henderson and Demond [11]. An extensive mass balance analysis of aqueous  
331 iron corrosion has been used to show that volumetric expansion is the major control on  
332 permeability loss. It has been shown that, whilst Fe<sup>0</sup> filtration systems (including PRBs)  
333 operating in anoxic (phreatic zone) conditions can exhibit limited permeability loss due to Fe<sup>0</sup>

334 corrosion product formation, Fe<sup>0</sup> filtration systems operating in oxic (vadose zone) conditions  
335 exhibit significantly high permeability loss. It can therefore be concluded that admixing Fe<sup>0</sup>  
336 with a non expansive materials (e.g. gravel, MnO<sub>2</sub>, pumice, sand) is a prerequisite for any  
337 sustainable Fe<sup>0</sup> filtration systems operating in the near surface geosphere.

338 The present work and related studies have delineated the early development of the Fe<sup>0</sup> PRB  
339 technology that was marked by empirical designs [37,38,74,75-80]. Field experiences from  
340 more than 120 reactive barriers and an innumerable numbers of filters (including laboratory  
341 columns) worldwide should be used to continuously refine this innovative technology.

342 Clearly the Fe<sup>0</sup> technology should now be translated into rational engineering design criteria.  
343 As there are no established comprehensive design criteria for Fe<sup>0</sup> beds, the reproducibility and  
344 comparison of available results is problematic. For example, despite the established  
345 significance of particle shape and size on the permeability, these parameters are not routinely  
346 given when describing operational conditions. Similarly, the initial porosity is not always  
347 given and the contribution of iron corrosion products to its filling was not properly addressed.

348 A tentative guideline for future laboratory experiments can also be concluded: (i) assess the  
349 intrinsic reactivity of used Fe<sup>0</sup>, (ii) define the size and sphericity of all used materials (Fe<sup>0</sup> and  
350 admixing materials), (iii) consider the surface roughness of Fe<sup>0</sup> and sand grains, (iv)  
351 characterize the dimension and the composition of used columns, (v) evaluate the porosity of  
352 resulted columns, (vi) characterize used initial solutions (e.g. pH, Eh, O<sub>2</sub> level,  
353 contamination), (vii) record the time dependant volume of the column effluent, and (viii)  
354 characterize the column effluent for pH, Eh, dissolved iron, target contaminants.

### 355 **Acknowledgments**

356 The manuscript was improved by the insightful comments of anonymous reviewers from  
357 CLEAN Soil, Air, Water.

### 358 **References**

359 [1] D. Blowes, Tracking hexavalent Cr in groundwater. *Science* **2002**, 295, 2024–2025.

- 360 [2] J.L. Jambor, M. Raudsepp, K. Mountjoy, Mineralogy of permeable reactive barriers for  
361 the attenuation of subsurface contaminants. *Can. Miner.* **2005**, *43*, 2117–2140.
- 362 [3] K. Komnitsas, G. Bartzas, I. Paspaliaris, Inorganic contaminant fate assessment in zero-  
363 valent iron treatment walls. *Environ. Forensics* **2006**, *7*, 207–217.
- 364 [4] K. Komnitsas, G. Bartzas, I. Paspaliaris, Modeling of reaction front progress in fly ash  
365 permeable reactive barriers. *Environ. Forensics* **2006**, *7*, 219–231.
- 366 [5] A.D. Henderson, A.H. Demond, Long-term performance of zero-valent iron permeable  
367 reactive barriers: a critical review. *Environ. Eng. Sci.* **2007**, *24*, 401–423.
- 368 [6] A.B. Cundy, L. Hopkinson, R.L.D. Whitby, Use of iron-based technologies in  
369 contaminated land and groundwater remediation: A review. *Sci. Tot. Environ.* **2008**,  
370 *400*, 42–51.
- 371 [7] R. Thiruvengkatachari, S. Vigneswaran, R. Naidu, Permeable reactive barrier for  
372 groundwater remediation. *J. Ind. Eng. Chem.* **2008**, *14*, 145–156.
- 373 [8] S. Comba, A. Di Molfetta, R. Sethi, A Comparison between field applications of nano-,  
374 micro-, and millimetric zero-valent iron for the remediation of contaminated aquifers.  
375 *Water Air Soil Pollut.* **2011**, *215*, 595–607.
- 376 [9] M. Gheju, Hexavalent chromium reduction with zero-valent iron (ZVI) in aquatic systems.  
377 *Water Air Soil Pollut.* **2011**, *222*, 103–148.
- 378 [10] ITRC, Permeable reactive barrier: Technology update. PRB-5. Washington, D.C.:  
379 Interstate Technology & Regulatory Council, PRB: Technology Update Team (**2011**).  
380 [www.itrcweb.org](http://www.itrcweb.org) (access: 09.03.2012)
- 381 [11] A.D. Henderson, A.H. Demond, Impact of solids formation and gas production on the  
382 permeability of ZVI PRBs. *J. Environ. Eng.* **2011**, *137*, 689–696.
- 383 [12] N. Muchitsch, T. Van Nooten, L. Bastiaens, P. Kjeldsen, Integrated evaluation of the  
384 performance of a more than seven year old permeable reactive barrier at a site

385 contaminated with chlorinated aliphatic hydrocarbons (CAHs). *J. Contam. Hydrol.*  
386 **2011**, *126*, 258–270.

387 [13] S. Ulsamer, A model to characterize the kinetics of dechlorination of tetrachloroethylene  
388 and trichloroethylene by a zero valent iron permeable reactive barrier. Master thesis,  
389 Worcester Polytechnic Institute, **2011**, 73 pp.

390 [14] E. Bi, J.F. Devlin, B. Huang, Effects of mixing granular iron with sand on the kinetics of  
391 trichloroethylene reduction. *Ground Water Monit. Remed.* **2009**, *29*, 56–62.

392 [15] Y.H. Kim, S.-O. Ko, H.C. Yoo, Simultaneous removal of tetrachlorocarbon and  
393 chromium(VI) using zero valent iron. *J. Korean Soc. Environ. Eng.* **2002**, *24*, 1949–  
394 1956.

395 [16] D.-I. Song, Y.H. Kim, W.S. Shin, A simple mathematical analysis on the effect of sand  
396 in Cr(VI) reduction using zero valent iron. *Korean J. Chem. Eng.* **2005**, *22*, 67–69.

397 [17] N. Moraci, P.S. Calabrò, Heavy metals removal and hydraulic performance in zero-  
398 valent iron/pumice permeable reactive barriers. *J. Environ. Manage.* **2010**, *91*, 2336–  
399 2341.

400 [18] G. Bartzas, K. Komnitsas, Solid phase studies and geochemical modelling of low-cost  
401 permeable reactive barriers. *J. Hazard. Mater.* **2010**, *183*, 301–308.

402 [19] L. Li, C.H. Benson, Evaluation of five strategies to limit the impact of fouling in  
403 permeable reactive barriers. *J. Hazard. Mater.* **2010**, *181*, 170–180.

404 [20] M.S. Odziemkowski, T.T. Schuhmacher, R.W. Gillham, E.J. Reardon, Mechanism of  
405 oxide film formation on iron in simulating groundwater solutions: Raman  
406 spectroscopic studies. *Corros. Sci.* **1998**, *40*, 371–389.

407 [21] S. Yabusaki, K. Cantrell, B. Sass, C. Steefel, Multicomponent reactive transport in an in  
408 situ zero-valent iron cell. *Environ. Sci. Technol.* **2001**, *35*, 1493–1503.



- 409 [22] R. Venkatapathy, D.G. Bessingpas, S. Canonica, J.A. Perlinger, Kinetic models for  
410 trichloroethylene transformation by zero-valent iron. *Appl. Catal. Environ.* **2002**, *37*,  
411 139–159.
- 412 [23] R.T. Wilkin, R.W. Puls, G.W. Sewell, Long-term performance of permeable reactive  
413 barriers using zero-valent iron: Geochemical and microbiological effects. *Ground*  
414 *Water* **2002**, *41*, 493–503.
- 415 [24] R.L. Johnson, R.B. Thoms, R.O'B. Johnson, T. Krug, Field evidence for flow reduction  
416 through a zero-valent iron permeable reactive barrier. *Ground Water Monit. Remed.*  
417 **2008**, *28*, 47–55.
- 418 [25] R.L. Johnson, R.B. Thoms, R.O'B. Johnson, J.T. Nurmi, P.G. Tratnyek, Mineral  
419 precipitation upgradient from a zero-valent iron permeable reactive barrier. *Ground*  
420 *Water Monit. Remed.* **2008**, *28*, 56–64.
- 421 [26] M. Odziemkowski, Spectroscopic studies and reactions of corrosion products at surfaces  
422 and electrodes. *Spectrosc. Prop. Inorg. Organomet. Compd.* **2009**, *40*, 385–450.
- 423 [27] S.W. Orth, R.W. Gillham, Dechlorination of trichloroethene in aqueous solution using  
424 Fe<sup>0</sup>. *Environ. Sci. Technol.* **1996**, *30*, 66–71.
- 425 [28] Y. Zhang, R.W. Gillham, Effects of gas generation and precipitates on performance of  
426 Fe<sup>0</sup> PRBs. *Ground Water* **2005**, *43*, 113–121.
- 427 [29] M.J. Wildman, P.J.J. Alvarez, RDX degradation using an integrated Fe(0)-microbial  
428 treatment approach. *Water Sci. Technol.* **2001**, *43*, 25–33.
- 429 [30] S. Biswas, P. Bose, Zero-valent iron assisted autotrophic denitrification. *J. Environ. Eng.*  
430 *ASCE* **2005**, *131*, 1212–1220.
- 431 [31] S.-M. Wang, S.-k. Tseng, Reductive dechlorination of trichloroethylene by combining  
432 autotrophic hydrogen-bacteria and zero-valent iron particles. *Biores. Technol.* **2009**,  
433 *100*, 111–117.

- 434 [32] T. Van Nooten, D. Springael, L. Bastiaens, Positive impact of microorganisms on the  
435 performance of laboratory-scale permeable reactive iron barriers. *Environ. Sci.*  
436 *Technol.* **2008**, 42, 1680–1686.
- 437 [33] N.B. Pilling, R.E. Bedworth, The oxidation of metals at high temperatures. *J. Inst. Metals*  
438 **1923**, 29, 529–591.
- 439 [34] K. Suda, S. Misra, K. Motohashi, Corrosion products of reinforcing bars embedded in  
440 concrete. *Corros. Sci.* **1993**, 35, 1543–1549.
- 441 [35] S. Caré, Q.T. Nguyen, V. L'Hostis, Y. Berthaud, Mechanical properties of the rust layer  
442 induced by impressed current method in reinforced mortar. *Cement Concrete Res.*  
443 **2008**, 38, 1079–1091.
- 444 [36] Y. Zhao, H. Ren, H. Dai, W. Jin, Composition and expansion coefficient of rust based on  
445 X-ray diffraction and thermal analysis. *Corros. Sci.* **2011**, 53, 1646–1658.
- 446 [37] C. Noubactep, Aqueous contaminant removal by metallic iron: Is the paradigm shifting?  
447 *Water SA* **2011**, 37, 419–426.
- 448 [38] C. Noubactep, S. Caré, K.B.D. Btatkeu, C.P. Nansou-Njiki, Enhancing the sustainability  
449 of household Fe<sup>0</sup>/sand filters by using bimetals and MnO<sub>2</sub>. *Clean – Soil, Air, Water*  
450 **2012**, 40, 100–109.
- 451 [39] G.H. Brimhall, J.L. Christopher, C. Ford, J. Bratt, G. Taylor, O. Warin, Quantitative  
452 geochemical approach to pedogenesis: importance of parent material reduction,  
453 volumetric expansion, and eolian influx in lateritization. *Geoderma* **1991**, 51, 51–91.
- 454 [40] R. Balasubramaniam, K.A.V. Ramesh, P. Dillmann, Characterization of rust on ancient  
455 Indian iron. *Curr. Sci.* **2003**, 85, 1546–1555.
- 456 [41] M. Kubare, J. Haarhoff, Rational design of domestic biosand filters. *J. Water Supply:*  
457 *Res. Technol. – AQUA* **2010**, 59, 1–15.
- 458 [42] K.P. Panayiotopoulos, Packing of sands - a review. *Soil Tillage Res.* **1989**, 13, 101–121.

- 459 [43] J. Haarhoff, A. Vessal, A falling-head procedure for the measurement of filter media  
460 sphericity. *Water SA* **2010**, 36, 97–104.
- 461 [44] K.-M. Yao, M.T. Habibian, C.R. O’melia, Water and waste water filtration: concepts and  
462 applications. *Environ. Sci. Technol.* **1971**, 5, 1105–1112.
- 463 [45] P. Bedrikovetsky, F.D. Siqueira, C.A. Furtado, A.L.S. Souza, Modified particle  
464 detachment model for colloidal transport in porous media. *Transp. Porous Med.* **2011**,  
465 86, 353–383.
- 466 [46] W.O. Smith, P.D. Foote, P.F. Busang, Packing of homogeneous spheres. *Phys. Rev.*  
467 **1929**, 34, 1271–1274.
- 468 [47] E. Manegold, R. Hofmann, K. Solf, Ueber Kapillarsysteme XII. I. Die mathematische  
469 Behandlung idealer Kugelpackungen und das Hohlraumvolumen realer  
470 Gerüststrukturen. *Colloid Polymer Sci.* **1931**, 56, 142–159.
- 471 [48] H. Iwata, T. Homma, Distribution of coordination numbers in random packing of  
472 homogeneous spheres. *Powder Technol.* **1994**, 10, 79–83.
- 473 [49] Neto, L.N., Kotousov, A. & Bedrikovetsky, P. Application of contact theory to  
474 evaluation of elastic properties of low consolidated porous media. *Int. J. Fract.* **2011**,  
475 168, 267–276.
- 476 [50] A. Hussam, A.K.M. Munir, A simple and effective arsenic filter based on composite iron  
477 matrix: Development and deployment studies for groundwater of Bangladesh. *J.*  
478 *Environ. Sci. Health A* **2007**, 42, 1869–1878.
- 479 [51] M.A. Shannon, P.W. Bohn, M. Elimelech, J.G. Georgiadis, B.J. Marinas, A.M.  
480 Mayes, Science and technology for water purification in the coming decades. *Nature*  
481 **2008**, 452, 301–310.
- 482 [52] C. Noubactep, Metallic iron for safe drinking water worldwide. *Chem. Eng. J.* **2010**, 165,  
483 740–749.

- 484 [53] D.E. Giles, M. Mohapatra, T.B. Issa, S. Anand, P. Singh, Iron and aluminium based  
485 adsorption strategies for removing arsenic from water. *J. Environ. Manage.* **2011**, *92*,  
486 3011–3022.
- 487 [54] H. Darcy, Les fontaines publiques de la Ville de Dijon. V. Dalmont, Paris (1856) 647 pp.
- 488 [55] T.O. Mahlangu, B.B. Mamba, M.N.B. Momba, A comparative assessment of chemical  
489 contaminant removal by three household water treatment filters. *Water SA* **2012**, *38*,  
490 39–48.
- 491 [56] C.E. Stauber, E.R. Printy F.A. McCarty, K.R. Liang, M.D. Sobsey, Cluster randomized  
492 controlled trial of the plastic biosand water filter in Cambodia. *Environ. Sci. Technol.*  
493 **2012**, *46*, 722–728.
- 494 [57] M. Lea, Biological sand filters: Low-cost bioremediation technique for production of  
495 clean drinking water. *Current Protocols Microbiol.* 1G.1.1-1G.1.28 **2008**, doi:  
496 10.1002/9780471729259.mc01g01s9.
- 497 [58] C. Noubactep, Processes of contaminant removal in “Fe<sup>0</sup>–H<sub>2</sub>O” systems revisited. The  
498 importance of co-precipitation. *Open Environ. J.* **2007**, *1*, 9–13.
- 499 [59] C. Noubactep, A critical review on the mechanism of contaminant removal in Fe<sup>0</sup>–H<sub>2</sub>O  
500 systems. *Environ. Technol.* **2008**, *29*, 909–920.
- 501 [60] C. Noubactep, The suitability of metallic iron for environmental remediation. *Environ.*  
502 *Progr. Sust. En.* **2010**, *29*, 286–291.
- 503 [61] C. Noubactep, The fundamental mechanism of aqueous contaminant removal by metallic  
504 iron. *Water SA* **2010**, *36*, 663–670.
- 505 [62] M. Edwards, M. Benjamin, Adsorptive filtration using coated sand: A new approach for  
506 treatment of metal-bearing wastes. *J. Water Pollut. Control Fed.* **1989**, *61*, 1523–1533.
- 507 [63] A.H. Khan, S.B. Rasul, A.K.M. Munir, M. Habibuddowla, M. Alauddin, S.S. Newaz, A.  
508 Hussam, Appraisal of a simple arsenic removal method for groundwater of Bangladesh.  
509 *J. Environ. Sci. Health A* **2000**, *35*, 1021–1041.

- 510 [64] D. Dermatas, X. Meng, Removal of As, Cr and Cd by adsorptive filtration. *Global Nest:*  
511 *the Int. J.* **2004**, 6, 73–80.
- 512 [65] S. Roy, P. Bose, Modeling arsenite adsorption on rusting metallic iron. *J. Environ. Eng.*  
513 **2010**, 136, 405–411.
- 514 [66] K. Hanna, Adsorption of aromatic carboxylate compounds on the surface of synthesized  
515 iron oxide-coated sands. *Appl. Geochem.* **2007**, 22, 2045–2053.
- 516 [67] K. Hanna, Sorption of two aromatic acids onto iron oxides: Experimental study and  
517 modeling. *J. Colloid Interf. Sci.* **2007**, 309, 419–428.
- 518 [68] K. Eusterhues, F.E. Wagner, W. Häusler, M. Hanzlik, H. Knicker, K.U. Totsche, I.  
519 Kögel-Knabner, U. Schwertmann, Characterization of ferrihydrite-soil organic matter  
520 coprecipitates by X-ray diffraction and Mössbauer spectroscopy. *Environ. Sci. Technol.*  
521 **2008**, 42, 7891–7897.
- 522 [69] K. Hanna, J.-F. Boily, Sorption of two naphthoic acids to goethite surface under flow  
523 through conditions. *Environ. Sci. Technol.* **2010**, 44, 8863–8869.
- 524 [70] K. Eusterhues, T. Rennert, H. Knicker, I. Kögel-Knabner, K.U. Totsche, U. Schwertmann,  
525 Fractionation of organic matter due to reaction with ferrihydrite: Coprecipitation versus  
526 adsorption. *Environ. Sci. Technol.* **2011**, 45, 527–533.
- 527 [71] B. Saha, S. Das, J. Saikia, G. Das, Preferential and enhanced adsorption of different dyes  
528 on iron oxide nanoparticles: A comparative study. *J. Phys. Chem. C* **2011**; 115, 8024–  
529 8033.
- 530 [72] U. Förstner, P. Jacobs, F. v. d. Kammer, Impact of natural nanophases on heavy-metal  
531 retention in zeolite-supported reactive filtration facilities for urban run-off treatment.  
532 *Fresenius J. Anal. Chem.* **2001**, 371, 652–659.
- 533 [73] C. Noubactep, T. Licha, T.B. Scott, M. Fall, M. Sauter, Exploring the influence of  
534 operational parameters on the reactivity of elemental iron materials. *J. Hazard. Mater.*  
535 **2009**, 172, 943–951.

- 536 [74] A. Ghauch, H. Abou Assi, H. Baydoun, A.M. Tuqan, A. Bejjani, Fe<sup>0</sup>-based trimetallic  
537 systems for the removal of aqueous diclofenac: Mechanism and kinetics. *Chem. Eng.*  
538 *J.* **2011**, *172*, 1033–1044.
- 539 [75] R.A. Crane, T.B. Scott, Nanoscale zero-valent iron: future prospects for an emerging  
540 water treatment technology. *J. Hazard. Mater.* **2012**, *211–212*, 112–125.
- 541 [76] C. Noubactep, S. Caré, R.A. Crane, Nanoscale metallic iron for environmental  
542 remediation: prospects and limitations. *Water Air Soil Pollut.* **2012**, *223*, 1363–1382.
- 543 [77] C. Noubactep, Metallic iron for water treatment: A knowledge system challenges  
544 mainstream science. *Fresenius Environ. Bull.* **2011**, *20*, 2632–2637.
- 545 [78] C. Noubactep, E. Temgoua, M.A. Rahman, Designing iron-amended biosand filters for  
546 decentralized safe drinking water provision. *Clean: Soil, Air, Water* **2012**, doi:  
547 10.1002/clen.201100620.
- 548 [79] C. Noubactep, Investigating the processes of contaminant removal in Fe<sup>0</sup>/H<sub>2</sub>O systems.  
549 *Korean J. Chem. Eng.* **2012**, doi: 10.1007/s11814-011-0298-8.
- 550 [80] R. Crane, C. Noubactep, Elemental metals for environmental remediation: learning from  
551 hydrometallurgy. *Fresenius Environ. Bull.* **2012**, *21*, 1192–1196.
- 552
- 553

553 **Table 1:** Some characteristics of metallic iron ( $\text{Fe}^0$ ) and its main corrosion products  
 554 commonly identified in  $\text{Fe}^0$  PRBs. “x” is the weight percent of Fe in the phase. As a  
 555 rule, oxides formed under anoxic conditions exhibit larger x values. “ $\eta$ ” is the  
 556 calculated coefficient of volumetric expansion. Phase parameters are compiled from  
 557 Balasubramaniam et al. [40] and Henderson and Demond [11].

558

Phase	Name	Structure	Density ( $\text{g}/\text{cm}^3$ )	$V_m$ ( $\text{cm}^3/\text{mol}$ )	x (%)	$\eta$ (-)
$\text{Fe}^0$	Iron metal	bcc	7.86	7.6	100.0	-
$\text{Fe}(\text{OH})_3$	$\text{Fe}^{\text{III}}$ hydroxide	perovskite-like	3.1	34.4	52.0	4.53
$\text{FeCO}_3$	Siderite	Trigonal	3.83	29.3	48.3	3.86
$\text{Fe}(\text{OH})_2$	$\text{Fe}^{\text{II}}$ hydroxide	Trigonal	3.4	26.4	62.2	3.47
$\alpha\text{-FeOOH}$	Goethite	Orthorhombic	4.28	20.3	62.9	2.67
$\gamma\text{-Fe}_2\text{O}_3$	Maghemite	Cubic	4.69	29.1	70.0	1.91
$\alpha\text{-Fe}_2\text{O}_3$	Hematite	Trigonal	5.3	30.1	70.0	1.98
$\text{Fe}_3\text{O}_4$	Magnetite	Cubic	5.175	45.0	72.4	1.97

559

560

561

561 **Table 2:** Estimation of the extent of Fe<sup>0</sup> depletion ( $\alpha$  value in %) in the column of Henderson  
 562 and Demond [11] for two values of the initial bed porosity.  $\alpha$  and  $\alpha_1$  correspond to  $\Phi_0 = 36$  %  
 563 when H<sub>2</sub> remains in the system or escapes respectively and  $\alpha'$  and  $\alpha'_1$  correspond to  $\Phi_0 = 62$   
 564 % when H<sub>2</sub> remains in the system or escapes respectively. It is seen that in all cases the initial  
 565 porosity is filled by gas when less than 0.1 % of the initial mass of Fe<sup>0</sup> is corroded. A value of  
 566 100 % is related to a system which is not clogged when Fe<sup>0</sup> is depleted.

567

568

Name	Formula	$\alpha$ values (%)			
		$\alpha$	$\alpha_1$	$\alpha'$	$\alpha'_1$
Maghemite	Fe <sub>2</sub> O <sub>3</sub>	0.01	62	0.04	100
Magnetite	Fe <sub>3</sub> O <sub>4</sub>	0.01	58	0.04	100
Hematite	Fe <sub>2</sub> O <sub>3</sub>	0.01	57	0.04	100
Goethite	FeOOH	0.02	34	0.06	98
Ferrous hydroxide	Fe(OH) <sub>2</sub>	0.02	24	0.06	70
Siderite	FeCO <sub>3</sub>	0.02	20	0.06	57
Ferric hydroxide	Fe(OH) <sub>3</sub>	0.02	16	0.06	46

569

570



570 **Figure captions**

571

572 **Figure 1:** Comparison of the evolution of porosity loss in a  $\text{Fe}^0$  bed filled with spherical (left)  
573 and cylindrical (right) particles. The compactness is maximal for spherical  
574 particles. The roundness or sphericity of used materials ( $\text{Fe}^0$  and additives) should  
575 be routinely characterized as this is crucial for the initial porosity.

576 **Figure 2:** Types of  $\text{Fe}^0$ -based filters for water treatment. The point O(0.0) represents a  $\text{Fe}^0$   
577 free filter (e.g. biosand filter, iron oxide-amended sand). The point I(100,100)  
578 correspond to a filter which is clogged just at  $\text{Fe}^0$  depletion.

579 **Figure 3:** Evolution of the residual porosity as function of the volumetric proportion of  $\text{Fe}^0$  is  
580 the filter for the two extreme values of the initial porosity ( $\Phi_0 = 0.36$  and  $0.62$ ). It is  
581 seen that for  $\Phi_0 = 0.36$  no filter is sustainable. For  $\Phi_0 = 0.62$ , filter operating under  
582 strictly anoxic conditions are sustainable.